711-02
194177
p.34

NASA TN D-24

TECHNICAL NOTE

D-24

CALCULATION OF SUPERSONIC FLOW PAST BODIES SUPPORTING SHOCK WAVES SHAPED LIKE ELLIPTIC CONES

By Benjamin R. Briggs

Ames Research Center
Moffett Field, Calif.

(NASA-TN-D-24) CALCULATION OF SUPERSONIC FLOW PAST BODIES SUPPORTING SHOCK WAVES SHAPED LIKE ELLIPTIC CONES (NASA. Ames Research Center) 34 p

N89-71290

Unclas
00/02 0194177

NATIONAL AERONAUTICS AND SPACE ADMINISTRATION
WASHINGTON August 1959

Y

NATIONAL AERONAUTICS AND SPACE ADMINISTRATION

TECHNICAL NOTE D-24

CALCULATION OF SUPERSONIC FLOW PAST BODIES SUPPORTING SHOCK WAVES SHAPED LIKE ELLIPTIC CONES

By Benjamin R. Briggs

SUMMARY

Numerical solutions are presented for supersonic perfect-gas flow past bodies which support shock waves shaped like elliptic cones. The full inviscid equations of motion are applied. The inverse method of solution is used, wherein the conditions at the shock wave are prescribed and the results are in the form of body shapes and surface pressure distributions. Comparisons are made with existing approximate theories and with results for circular cones.

INTRODUCTION

In the past most of the attempts to obtain usable solutions for two- or three-dimensional supersonic flow problems have been of an approximate nature. Through the use of high-speed electronic computers, however, solutions have been obtained using the full inviscid equations of motion. An example is the solution of the problem of a blunt body in a supersonic stream by numerical means (see refs. 1 and 2).

The numerical technique employed in references 1 and 2 was to prescribe the shape of the detached shock wave, and then to locate the body by integrating inwardly and finding where a stream function vanished. It was suggested in reference 2 that the same general numerical methods, along with the use of a pair of stream functions, might be employed in solving three-dimensional flow problems. The use of two (or more) stream functions in three-dimensional flows is discussed in reference 3.

Another problem which has been solved numerically using the full inviscid equations of motion is the supersonic flow past circular cones at zero angle of attack (see ref. 4). Various approximate methods have been advanced for finding the flow properties of slightly noncircular cones, or circular cones at small angle of attack (see, e.g., refs. 5 and 6).

In supersonic flow an entropy layer exists over noncircular or yawed conical bodies. The value of entropy must be constant on the body. These concepts have been utilized in reference 7 to obtain body shape from a numerical study of the entropy in the flow field behind a yawed circular-cone shock. In addition to the entropy layer, singularities in the entropy appear on the conical bodies when the conical body is noncircular or yawed (see refs. 6 and 8).

In the present paper supersonic conical flow past bodies that support shock waves shaped like elliptic cones is studied numerically. The technique of prescribing the shock-wave shape (refs. 1, 2, and 7) is employed. The full inviscid equations of motion are used, and the problem is formulated in terms of two stream functions.

The author is indebted to Dr. Milton D. Van Dyke who originally posed the problem reported here and suggested how to use two stream functions in the analysis.

SYMBOLS

a,b	semimajor and semiminor axes of elliptic cross section of coordinate surfaces of constant θ (eqs. (2b), (3))
a_1,b_1	semimajor and semiminor axes of elliptic cross section of coordinate surfaces of constant ϕ (eqs. (2c), (3))
A,B,C,D	functions defined in equations (7)
c_1,c_2	constants in equations (11b) which specify stream surfaces
f,g	stream functions of a three-dimensional flow
F,G	specializations of f and g for the present conical-flow problem
h_1,h_2,h_3	coefficients in the metric of the sphero-conal coordinate system
k^2,k'^2	constants in the sphero-conal coordinate transformation
M	Mach number
N	function defined in equation (33)
p	pressure referred to $\rho_\infty U_\infty{}^2$
r,θ,ϕ	sphero-conal coordinates
S	$\dfrac{p}{\rho^\gamma}$
u,v,w	velocities components in the sphero-conal coordinate system referred to U_∞

u_1, v_1, w_1 velocities in the directions x,y,z, respectively

U_∞ free-stream velocity

$\vec{V}$ vector having components u,v,w

x,y,z Cartesian coordinates

γ adiabatic exponent

$\Gamma(x,y,z)$ coordinate surface that coincides with the shock wave

$\Delta\theta, \Delta\phi$ increments of θ and ϕ which define the mesh width in the numerical calculations

ρ density referred to free-stream value

Subscripts

b condition on body surface

n nth extrapolation

N normal component (eq. (23))

o conditions on the shock wave

r,θ,ϕ differentiation with respect to variables r,θ, and ϕ

x,y,z x,y,z components of Mach number (eq. (23))

Superscripts

(n) nth extrapolation

' differentiation with respect to the variable G, encountered in the components of $\mathrm{grad}(\rho^\gamma S)$ in the directions r,θ,ϕ

EXAMINATION OF THE PROBLEM

The technique used here is similar to that employed in references 1 and 2. Initial flow data are calculated at a shock wave of prescribed shape, and then the body is found by integrating the equations of motion inwardly toward the body. In two-dimensional or axisymmetric flow problems, a function which represents the integral of the differential equation of the streamlines exists. This function is the well-known stream function. In the present three-dimensional analysis an important feature is the use of two such functions. A discussion of this generalization is given in reference 3. These two functions are constant on streamlines, and the intersection of surfaces represented by the functions are the streamlines. It is natural, then, to think of them as stream functions for the three-dimensional problem. The body is located where one of these two functions vanishes. Results of the calculations are body shape and surface pressure.

Following an exposition of the coordinate system, equations of motion, and initial conditions, a description of the numerical integration process is given. Several specific calculations are then discussed, including a comparison with circular-cone computations given in reference 4, and a comparison with the theory of reference 5 for slightly noncircular cones. The effect of varying the adiabatic exponent γ in a flow at very high Mach number is shown, and the limiting case of γ nearly one is compared with simple Newtonian theory.

The report is concluded with a discussion of the results and a mention of possible avenues of extension of the present method to include angles of attack or sideslip, and a closer study of the vorticity layer and entropy singularities which are known (see refs. 6 and 8) to exist on the surface of noncircular conical bodies or cones at angles of attack or sideslip.

THE SPHERO-CONAL COORDINATE SYSTEM

It is an essential requirement in the numerical method to be applied that the shock wave be a coordinate surface and in this case an elliptic cone. An orthogonal coordinate system r,θ,ϕ which meets this requirement is given in reference 9. This transformation from a Cartesian system x,y,z is

$$\left.\begin{aligned} x &= r\cos\theta\sqrt{1-k'^2\cos^2\phi} \\ y &= r\sin\theta\sin\phi \\ z &= r\cos\phi\sqrt{1-k^2\cos^2\theta} \\ k^2+k'^2 = 1\,, &\quad 0\leq\theta\leq\pi\,,\quad 0\leq\phi\leq 2\pi \end{aligned}\right\} \tag{1}$$

The coordinate system represented by equation (1) is called the sphero-conal system. Observe that for $k^2 = 1$ and $k'^2 = 0$ this system reduces to spherical polar coordinates about the x axis, and for $k^2 = 0$ and $k'^2 = 1$ it reduces to a spherical polar set about the z axis.

The coordinate surfaces of the system represented by equation (1) are spheres and two sets of elliptic cones, given by the following three equations.

$$x^2 + y^2 + z^2 = r^2 \,, \qquad \text{for fixed} \quad r = r_o \tag{2a}$$

$$x^2 - \frac{y^2}{\tan^2\theta} - \frac{z^2}{\dfrac{1-k^2\cos^2\theta}{k^2\cos^2\theta}} = 0 \,, \qquad \text{for fixed} \quad \theta = \theta_o \tag{2b}$$

$$\frac{x^2}{\dfrac{1-k'^2\cos^2\phi}{k'^2\cos^2\phi}} + \frac{y^2}{\tan^2\phi} - z^2 = 0 \,, \qquad \text{for fixed} \quad \phi = \phi_o \tag{2c}$$

Portions of the two sets of cones, equations (2b) and (2c), are shown in sketches (a) and (b).

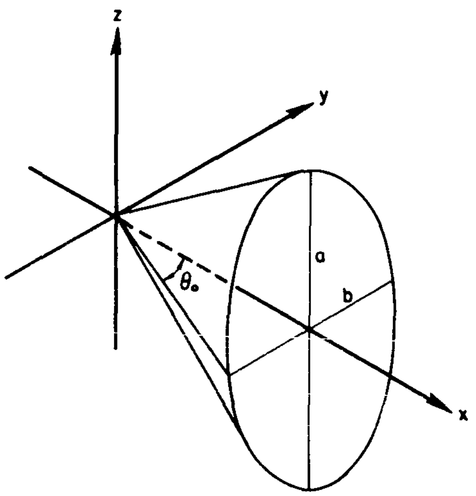

Sketch (a).- Constant θ

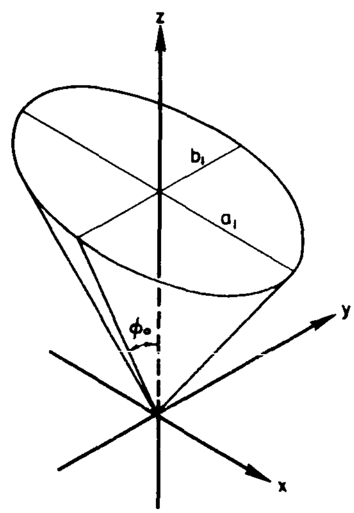

Sketch (b).- Constant ϕ

Points are defined at intersections of the cones and the spheres r = constant.

The semiminor and semimajor axes of the elliptic cross sections of the cones are shown in these sketches. In terms of the constants k^2, k'^2, θ_o, and ϕ_o, these may be written

$$\left.\begin{aligned}
a &= \sqrt{\frac{1-k^2\cos^2\theta_o}{k^2\cos^2\theta_o}} \\
b &= \tan\,\theta_o \qquad\qquad a \geq b \\
a_1 &= \sqrt{\frac{1-k'^2\cos^2\phi_o}{k'^2\cos^2\phi_o}} \\
b_1 &= \tan\,\phi_o \qquad\qquad a_1 \geq b_1
\end{aligned}\right\} \tag{3}$$

For the problem at hand it will be assumed that the prescribed shock wave is a cone of the family represented by equation (2b) (see sketch (a)). The free-stream flow will be in the direction of the positive x axis. The shock-wave geometry is fixed by giving constant values to θ and b/a. The constants k^2 and k'^2 can then be calculated from the relations

$$\left.\begin{aligned}
k^2 &= \frac{(b/a)^2}{\sin^2\theta_o + (b/a)^2\cos^2\theta_o} \\
k'^2 &= 1 - k^2
\end{aligned}\right\} \tag{4}$$

In the derivation of the equations of motion in terms of the orthogonal sphero-conal coordinates, the functions h_1^2, h_2^2, h_3^2, which are coefficients in the metric, are needed. The metric is given by

$$ds^2 = h_1^2 dr^2 + h_2^2 d\theta^2 + h_3^2 d\phi^2 \tag{5}$$

for orthogonal systems, and in the present case

$$\left.\begin{aligned}
h_1^2 &= 1 \\
h_2^2 &= r^2\,\frac{k^2\sin^2\theta + k'^2\sin^2\phi}{1 - k^2\cos^2\theta} \\
h_3^2 &= r^2\,\frac{k^2\sin^2\theta + k'^2\sin^2\phi}{1 - k'^2\cos^2\phi}
\end{aligned}\right\} \tag{6}$$

In the transformation of the equations of motion into the sphero-conal coordinates considerable simplification results when the following auxiliary functions are introduced:

$$
\left.
\begin{aligned}
A^2 &= \frac{1 - k^2\cos^2\theta}{k^2\sin^2\theta + k'^2\sin^2\phi} \\
B^2 &= \frac{1 - k'^2\cos^2\phi}{k^2\sin^2\theta + k'^2\sin^2\phi} \\
C &= \frac{k^2\sin\theta\cos\theta}{k^2\sin^2\theta + k'^2\sin^2\phi} \\
D &= \frac{k'^2\sin\phi\cos\phi}{k^2\sin^2\theta + k'^2\sin^2\phi} \\
\frac{\partial A}{\partial\theta} &= \frac{C(1-A^2)}{A} \qquad \frac{\partial B}{\partial\theta} = -BC \\
\frac{\partial A}{\partial\phi} &= -AD \qquad \frac{\partial B}{\partial\phi} = \frac{D}{B}(1-B^2)
\end{aligned}
\right\} \tag{7}
$$

Equation (6) can now be written in simpler form by use of relation (7); that is,

$$
h_1^2 = 1\ , \qquad h_2^2 = \frac{r^2}{A^2}\ , \qquad h_3^2 = \frac{r^2}{B^2} \tag{8}
$$

VELOCITIES IN THE SPHERO-CONAL SYSTEM

Velocity components u,v,w in the sphero-conal coordinates are defined in the following way. The component u is in the direction of the coordinate r. The velocities v and w are components along curves of constant ϕ and θ, respectively, on a spherical surface given by constant r. Sketch (c) illustrates curves of constant ϕ and θ, and the velocity components v and w are shown. It must be borne in mind that the sketch is a projected view of the spherical surface onto the y-z plane, and that the velocity components v and w do not lie in the y-z plane, but on a spherical surface.

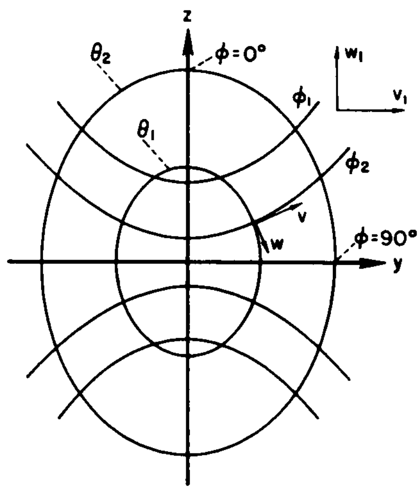

Sketch (c)

The relationship between the velocities u,v,w and the velocity components u_1,v_1,w_1 in the Cartesian coordinate system is given by the equations:

$$u_1 = \left(\sqrt{1-k'^2\cos^2\phi}\,\cos\theta\right)u - \left[\sqrt{\frac{(1-k^2\cos^2\theta)(1-k'^2\cos^2\phi)}{k^2\sin^2\theta+k'^2\sin^2\phi}}\,\sin\theta\right]v +$$

$$\left(\frac{k'^2\sin\phi\cos\phi\cos\theta}{\sqrt{k^2\sin^2\theta+k'^2\sin^2\phi}}\right)w$$

$$v_1 = (\sin\theta\sin\phi)u + \left(\sqrt{\frac{1-k^2\cos^2\theta}{k^2\sin^2\theta+k'^2\sin^2\phi}}\,\cos\theta\sin\phi\right)v +$$

$$\left(\sqrt{\frac{1-k'^2\cos^2\phi}{k^2\sin^2\theta+k'^2\sin^2\phi}}\,\sin\theta\cos\phi\right)w$$

$$w_1 = \left(\sqrt{1-k^2\cos^2\theta}\,\cos\phi\right)u + \left(\frac{k^2\sin\theta\cos\theta\cos\phi}{\sqrt{k^2\sin^2\theta+k'^2\sin^2\phi}}\right)v -$$

$$\left[\sqrt{\frac{(1-k^2\cos^2\theta)(1-k'^2\cos^2\phi)}{k^2\sin^2\theta+k'^2\sin^2\phi}}\,\sin\phi\right]w$$

THE EQUATIONS OF MOTION

General Remarks

The differential equations which describe the flow of an ideal perfect compressible fluid are, in vector form,

$$\operatorname{div}(\rho\vec{V}) = 0 \qquad \text{(continuity)} \tag{9a}$$

$$\rho(\vec{V}\cdot\operatorname{grad})\vec{V} + \operatorname{grad} p = 0 \qquad \text{(momentum)} \tag{9b}$$

$$\vec{V}\cdot\operatorname{grad}(p/\rho^\gamma) = 0 \qquad \text{(energy)} \tag{9c}$$

Here $\vec{V}$ is the velocity made dimensionless with respect to its free-stream value U_∞. The density ρ has been made dimensionless with reference to its free-stream value ρ_∞, and pressure p with respect to the quantity $\rho_\infty U_\infty^2$.

The Equations of Motion in the Sphero-Conal System

When equations (9) are transformed into the sphero-conal coordinate system, with the added assumption of conical flow, the results are

$$\frac{1}{B}\frac{\partial(\rho v)}{\partial\theta} + \frac{1}{A}\frac{\partial(\rho w)}{\partial\phi} + \rho\left(\frac{2u}{AB} + \frac{Cv}{B} + \frac{Dw}{A}\right) = 0 \tag{10a}$$

$$Av\frac{\partial u}{\partial\theta} + Bw\frac{\partial u}{\partial\phi} - (v^2+w^2) = 0 \tag{10b}$$

$$Av\frac{\partial v}{\partial\theta} + Bw\frac{\partial v}{\partial\phi} - ACw^2 + uv + BDvw + \frac{A}{\rho}\frac{\partial p}{\partial\theta} = 0 \tag{10c}$$

$$Av\frac{\partial w}{\partial\theta} + Bw\frac{\partial w}{\partial\phi} - BDv^2 + uw + ACvw + \frac{B}{\rho}\frac{\partial p}{\partial\phi} = 0 \tag{10d}$$

$$Av\frac{\partial(p/\rho^\gamma)}{\partial\theta} + Bw\frac{\partial(p/\rho^\gamma)}{\partial\phi} = 0 \tag{10e}$$

Here u, v, and w are velocities in the sphero-conal system, as discussed previously, and A, B, C, and D are defined in equation (7).

Equations (10) reduce to those for conical flow in ordinary spherical polar coordinates if values of 1 and 0 are taken for k^2 and k'^2, respectively (see, e.g., ref. 6). If the further stipulation of axisymmetric flow is made, then the velocity w vanishes and none of the remaining flow quantities vary with ϕ, and equations (10) reduce to those used in reference 4 in the direct circular-cone problem.

The Equations of Motion Written in Terms of Two Stream Functions

It is not convenient to use equations (10) in the numerical computations, as there is no way to infer the body shape from values of the velocities u, v, and w, and p and ρ in the flow field. In reference 3, three-deminsional flows are described by a method utilizing two functions which are integrals of the differential equations of the streamlines. One of these functions can be made to vanish at a solid boundary, such as the conical body of this analysis. This is a generalization of the stream function of two-dimensional or axisymmetric flows. The theory of reference 3 will be outlined here briefly.

Let u_1, v_1, w_1 be velocity components in the direction of the Cartesian coordinates x, y, z, respectively. Then the streamlines are given by the equations

$$\frac{dx}{u_1} = \frac{dy}{v_1} = \frac{dz}{w_1} \tag{11a}$$

Now, all of the integrals of these equations are contained in the two relations

$$\left.\begin{aligned} f_1(x,y,z) &= c_1 \\ g_1(x,y,z) &= c_2 \end{aligned}\right\} \tag{11b}$$

Stream surfaces are represented by these two equations for fixed values of the constants c_1 and c_2. The intersections of the stream surfaces f_1 and g_1 are streamlines, and it is clear then that f_1 and g_1 are constant on streamlines. The functions f_1 and g_1 are referred to as the stream functions for a three-dimensional flow. The velocities in terms of the two stream functions are represented by the vector product

$$\rho\vec{V} = (\text{grad } f_1) \times (\text{grad } g_1) \tag{12}$$

The energy equation then takes the simple form $p/\rho^\gamma = S(f_1, g_1)$ where S is related to the entropy of the flow field. The momentum equations can be written as

$$\rho(\vec{V}\cdot\text{grad})\vec{V} + \text{grad}[\rho^\gamma S(f_1, g_1)] = 0 \tag{13}$$

and the unknowns are now f_1, g_1, and ρ.

The velocities u, v, and w can be found in terms of f and g if equation (12) is transformed into the sphero-conal coordinate system. Thus,

$$\left.\begin{aligned} u &= \frac{AB}{\rho r^2}\left(f_\theta g_\phi - f_\phi g_\theta\right) \\ v &= \frac{B}{\rho r}\left(f_\phi g_r - f_r g_\phi\right) \\ w &= \frac{A}{\rho r}\left(f_r g_\theta - f_\theta g_r\right) \end{aligned}\right\} \tag{14}$$

Here f and g are understood to be functions of the coordinates r, θ, ϕ, and subscripts r, θ, and ϕ, indicate partial differentiation with respect to the variables r, θ, and ϕ, respectively. Observe that the assumption of conical flow has not been made in equation (14).

The theory summarized in the foregoing paragraphs will now be applied to the problem at hand. For conical flow $\vec{V}$, ρ, and S are not functions of the coordinate r. Thus the product fg must be homogeneous of order 2 in r (see eqs. (14)). In order that f will reduce to Stokes' stream function in the axisymmetric case, and also that the body be described by $f = 0$, it is convenient to let f be homogeneous of order 2 and g of order 0 in r. Thus, for conical flow, the transformation

$$\left.\begin{aligned} f(r,\theta,\phi) &= r^2F(\theta,\phi) \\ g(r,\theta,\phi) &= G(\theta,\phi) \end{aligned}\right\} \tag{15}$$

can be made. Then $S(f,g)$ cannot be independent of r unless it is also independent of f. Therefore,

$$S(f,g) = S(G) \tag{16}$$

Equation (14) can now be written in terms of F and G.

$$u = \frac{AB}{\rho}\left(F_\theta G_\phi - F_\phi G_\theta\right) \tag{17a}$$

$$v = -\frac{2B}{\rho} FG_\phi \tag{17b}$$

$$w = \frac{2A}{\rho} FG_\theta \tag{17c}$$

The components of $\text{grad}[\rho^\gamma S(G)]$ are

$$\left.\begin{aligned} &0 \\ &\frac{A\rho^\gamma S}{r}\left(\frac{r\rho_\theta}{\rho} + \frac{S'}{S}\, G_\theta\right) \\ &\frac{B\rho^\gamma S}{r}\left(\frac{r\rho_\phi}{\rho} + \frac{S'}{S}\, G_\phi\right) \end{aligned}\right\} \tag{18}$$

in the r, θ, and ϕ directions. The quantity $(\vec{V}\cdot\text{grad})\vec{V}$ in equation (13) can be written in terms of the component velocities u,v,w, as was done in the equations of motion, equations (10a), (10b), and (10c). Then, by use of equations (17) and (18) the equations of motion become:

θ momentum:

$$[\gamma\rho^{\gamma+1}S-(2BFG_\phi)^2]\left(\frac{\rho_\theta}{\rho}\right)$$

$$= (2BF)^2(G_\theta G_{\phi\phi}-G_\phi G_{\phi\theta}) - (\rho^{\gamma+1}S)\left(\frac{S'}{S}\right)G_\theta + 2B^2FG_\phi(F_\phi G_\theta - F_\theta G_\phi) +$$

$$(2F)^2G_\theta\left(D-B^2\frac{\rho_\phi}{\rho}\right)G_\phi + (2F)^2C(B^2G_\phi^2+A^2G_\theta^2) \tag{19}$$

ϕ momentum:

$$(2AF)^2 G_\phi G_{\theta\theta} = 2A^2 F G_\theta (F_\phi G_\theta - F_\theta G_\phi) + (2AFG_\theta)^2 \left[G_{\theta\phi} - G_\theta \left(D + \frac{\rho_\phi}{\rho} \right) + G_\phi \frac{\rho_\theta}{\rho} \right] - (2F)^2 G_\phi (CG_\theta + B^2 D G_\phi) + \rho^{\gamma+1} S \left(\gamma \frac{\rho_\phi}{\rho} + \frac{S'}{S} G_\phi \right) \tag{20}$$

r momentum:

$$(ABG_\phi)^2 F_{\theta\theta} = (AB)^2 \left[F_\theta G_\theta G_{\phi\phi} - (F_\theta G_\phi + F_\phi G_\theta) G_{\theta\phi} + F_\phi G_\phi G_{\theta\theta} - G_\theta^2 F_{\phi\phi} + 2 G_\theta G_\phi F_{\theta\phi} \right] - 2F(A^2 G_\theta^2 + B^2 G_\phi^2) - (F_\phi G_\theta - F_\theta G_\phi) \left[B^2 \left(2A^2 C - C + A^2 \frac{\rho_\theta}{\rho} \right) G_\phi - A^2 \left(2B^2 D - D - B^2 \frac{\rho_\phi}{\rho} \right) G_\theta \right] \tag{21}$$

THE INITIAL CONDITIONS

The shock wave is taken to be an elliptic cone of the form described by equation (2b), and the fixed value of θ will be designated θ_o. The equation of this conical surface is

$$\Gamma(x,y,z) = x^2 - \frac{y^2}{b^2} - \frac{z^2}{a^2} = 0 \tag{22}$$

The component of free-stream Mach number M_∞ normal to the shock wave is, in general,

$$M_N = \frac{M_x(\partial\Gamma/\partial x) + M_y(\partial\Gamma/\partial y) + M_z(\partial\Gamma/\partial z)}{\sqrt{(\partial\Gamma/\partial x)^2 + (\partial\Gamma/\partial y)^2 + (\partial\Gamma/\partial z)^2}} \tag{23}$$

where M_x, M_y, M_z are the components of Mach number in the x, y, and z directions, respectively. When equation (22) and the condition that $M_y = M_z = 0$ are used equation (23) becomes

$$M_N = M_\infty \sin\,\theta_o \sqrt{\frac{(1-k^2\cos^2\theta_o)(1-k'^2\cos^2\phi)}{k^2\sin^2\theta_o + k'^2\sin^2\phi}} \tag{24}$$

The pressure, density, and velocity behind the shock wave are

$$p = \frac{2\gamma M_N^2 - (\gamma-1)}{(\gamma+1)\gamma M_\infty^2} \tag{25a}$$

$$\rho = \frac{(\gamma+1)M_N^2}{(\gamma-1)M_N^2 + 2} \tag{25b}$$

$$v = -\frac{(\gamma-1)M_N^2 + 2}{(\gamma+1)M_N M_\infty} \tag{25c}$$

(see, e.g., ref. 10, eqs. (93), (94), and (96)). The velocities u and w are tangent to the shock, so they undergo no change through the shock. These velocities are

$$u = \cos\theta_0 \sqrt{1 - k'^2\cos^2\phi} \tag{25d}$$

$$w = \frac{k'^2\cos\theta_0\sin\phi\cos\phi}{\sqrt{k^2\sin^2\theta_0+k'^2\sin^2\phi}} \tag{25e}$$

There is still some freedom left in the choice of the form of the stream functions F and G. If it is specified that F be independent of ϕ at the shock wave the result is that it is a constant there. The value of this constant is specified, now, by requiring that G reduce to ϕ in the axisymmetric case. Using equations (24), (25b), (25c), and (7) in equation (17b) gives

$$\begin{aligned}\rho v &= -\frac{2\sqrt{1-k'^2\cos^2\phi}}{\sqrt{k^2\sin^2\theta_0+k'^2\sin^2\phi}}\,FG_\phi \\ &= -\sin\theta_0\,\frac{\sqrt{(1-k^2\cos^2\theta_0)(1-k'^2\cos^2\phi)}}{\sqrt{k^2\sin^2\theta_0+k'^2\sin^2\phi}}\end{aligned} \tag{26a}$$

Solving for G_ϕ results in the equation

$$G_\phi = \frac{\sin\theta_0\sqrt{1-k^2\sin^2\theta_0}}{2F} \tag{26b}$$

If F is chosen to be

$$F = \frac{\sin\theta_0\sqrt{1-k^2\cos^2\theta_0}}{2} \tag{27}$$

at the shock, then an integration of equation (26b) leads to

$$G = \phi \tag{28}$$

at $\theta = \theta_o$. In a similar manner equations (17a) and (17c) yield

$$F_\theta = \frac{2\rho F}{A^2 \tan \theta_o} \tag{29}$$

$$G_\theta = \frac{\rho D}{A^2 \tan \theta_o} \tag{30}$$

at the shock wave.

Equations for $S(G)$ and S'/S are needed, also. The required relations are

$$S(G) = \frac{2\gamma N^2 - (\gamma-1)}{\gamma(\gamma+1)M_\infty^2}\left[\frac{2 + (\gamma-1)N^2}{(\gamma+1)N^2}\right]^\gamma \tag{31}$$

$$\frac{S'}{S} = \frac{-4\gamma(\gamma-1)k^2k'^2\cos^2\theta_o(N^2-1)^2\sin G\cos G}{[2\gamma N^2-(\gamma-1)][2+(\gamma-1)N^2](k^2\sin^2\theta_o+k'^2\sin^2 G)(1-k'^2\cos^2 G)} \tag{32}$$

where

$$N^2(G) = \frac{M_\infty^2\sin^2\theta_o(1-k'^2\cos^2 G)(1-k^2\cos^2\theta_o)}{k^2\sin^2\theta_o + k'^2\sin^2 G} \tag{33}$$

THE NUMERICAL TECHNIQUE

The numerical problem is defined by equations (19) through (21), (25b), and (27) through (33). For a given case, values are specified for the following items.

$\left.\begin{array}{l}\theta_o\\ b/a\end{array}\right\}$ Shock-wave geometry

M_∞ Free-stream Mach number

γ Adiabatic exponent

$\left.\begin{array}{l}\Delta\theta\\ \Delta\phi\end{array}\right\}$ Mesh size

In practice, 20 points are picked in the region $0 < \phi < \pi/2$ on the shock wave. The starting value of ϕ is taken as 2.25°, and $\Delta\phi$ is 4.5°. Thus, the values of ϕ at which initial data are calculated are 2.25°, 6.75°, . . ., 87.75°. The value of $\Delta\theta$ is chosen so that at least 8 or 10 increments are taken to get to the body.

These computations have been programed for an ElectroData 205 Electronic Data Processing System having the automatic floating point feature. The program is arranged according to the following outline.

Step 1.- Compute initial values of ρ, F, G, F_θ, and G_θ for the 20 prescribed values of ϕ at the shock. Compute derivatives ρ_ϕ, F_ϕ, G_ϕ, $F_{\phi\phi}$, $G_{\phi\phi}$, $F_{\theta\phi}$, and $G_{\theta\phi}$ numerically. Compute $S(G)$, S'/S, ρ_θ, $G_{\theta\theta}$, and $F_{\theta\theta}$ from equations (31) through (33) and (19) through (21). Compute pressure using the relation $p = \rho^\gamma S$. The pertinent flow data, known now at the shock, are read out of the computer.

Step 2.- Extrapolate ρ, F_θ, and G_θ, known here at $\theta = \theta_n$, to the next value of θ, where $\theta_{n+1} = \theta_n - \Delta\theta$, using the formulas

$$\left.\begin{aligned} \rho^{(n+1)} &= \rho^{(n)} - \Delta\theta\ \rho_\theta^{(n)} \\ F_\theta^{(n+1)} &= F_\theta^{(n)} - \Delta\theta\ F_{\theta\theta}^{(n)} \\ G_\theta^{(n+1)} &= G_\theta^{(n)} - \Delta\theta\ G_{\theta\theta}^{(n)} \end{aligned}\right\} \tag{34}$$

Step 3.- Extrapolate F and G to the next smaller value of θ, namely θ_{n+1}, using the formulas

$$\left.\begin{aligned} F^{(n+1)} &= F^{(n)} - \Delta\theta\left[\frac{F_\theta^{(n)} + F_\theta^{(n+1)}}{2}\right] \\ G^{(n+1)} &= G^{(n)} - \Delta\theta\left[\frac{G_\theta^{(n)} + G_\theta^{(n+1)}}{2}\right] \end{aligned}\right\} \tag{35}$$

Note that $F_\theta^{(n+1)}$ and $G_\theta^{(n+1)}$, found in step 2, are used in step 3. The value of θ_{n+1} is now computed by use of the relation $\theta_{n+1} = \theta_n - \Delta\theta$.

Step 4.- Compute the derivatives ρ_ϕ, F_ϕ, G_ϕ, $F_{\phi\phi}$, $G_{\phi\phi}$, $F_{\theta\phi}$, and $G_{\theta\phi}$ numerically. Compute $S(G)$, S'/S, ρ_θ, $G_{\theta\theta}$, and $F_{\theta\theta}$ from equations (31) through (33) and (19) through (21). Pressure p is now found from the relation $p = \rho^\gamma S$. At this point, for the present value of θ, pertinent flow-field data for the prescribed 20 values of ϕ are read out of the computer.

Step 5.- If any values of F have become negative for the current set of data, for which $\theta = \theta_{n+1}$, then the previously calculated set at $\theta = \theta_n$ is recalled and the increment in θ to the body from θ_n is calculated for each value of ϕ by use of the relation

$$\Delta\theta_b = \frac{F_\theta^{(n)} - \sqrt{\left[F_\theta^{(n)}\right]^2 - 2F^{(n)}F_{\theta\theta}^{(n)}}}{F_{\theta\theta}^{(n)}} \tag{36}$$

and the coordinates y and z of the body cross section are found for $x = 1$ from the equations

$$\left.\begin{aligned} y_b &= \frac{\sin\phi \sin\theta_b}{\cos\theta_b\sqrt{1-k'^2\cos^2\phi}} \\ z_b &= \frac{\cos\phi\sqrt{1-k^2\cos^2\theta_b}}{\cos\theta_b\sqrt{1-k'^2\cos^2\phi}} \end{aligned}\right\} \tag{37}$$

where $\theta_b = \theta_n - \Delta\theta_b$. The pressure p is extrapolated to the body by use of the formula

$$p_b = p^{(n)} - \Delta\theta_b p_\theta^{(n)} \tag{38}$$

where

$$p_\theta^{(n)} = p^{(n)}\left[\gamma \frac{\rho_\theta^{(n)}}{\rho^{(n)}} + \left(\frac{S'}{S}\right)^{(n)} G_\theta^{(n)}\right] \tag{39}$$

The body coordinates and p_b are now read out of the computer and the case is finished.

If, on the other hand, all values of F are still positive here, at $\theta = \theta_{n+1}$, steps 2 through 4 are repeated. The repetition is carried out until F has changed sign, at which time the extrapolation to the body, as outlined in the foregoing paragraph, is carried out.

PRESENTATION OF RESULTS

Illustrative Examples

For illustrative purposes a case was studied for which the shock wave was defined by $\theta_o = 30^o$ and $b/a = 0.6$. The free-stream conditions were $M = 6$ and $\gamma = 1.4$. In order to assess the effect of the magnitude of the increment $\Delta\theta$ on the calculations, this example was computed for several values of $\Delta\theta$. The resulting body shapes (plotted in the $x = 1$ plane) and surface pressure distributions are shown in figures 1 and 2, respectively. Note that results are shown only for one-quarter of the body cross section. Pressures are plotted against the coordinate ϕ (see eqs. (1)). From equations (1) it is seen that where $\phi = 0^{\circ}$ on the body $y = 0$, and where $\phi = 90^{\circ}$ is where $z = 0$. Qualitatively, the body shape is more regular, particularly in the middle portion, for small values of $\Delta\theta$. The surface pressure distributions for the two smallest increments are indistinguishable from one another. To show in a somewhat more quantitative way that the calculations are stable and convergent, the body coordinate θ_b has been plotted against $\Delta\theta$ for several fixed values of ϕ (see fig. 3). It is evident that by taking smaller and smaller increments some final body shape is approached.

There is no reason to expect the body shape to be elliptic, in general. In the case under discussion, the body cross section is compared with an ellipse, namely the one through the points where $y = 0$ and $z = 0$ on the body (see fig. 4). The body is flatter than this ellipse in the middle portion, a not wholly unexpected result. Note that this is not a coordinate ellipse.

Another series of calculations was carried out using the same shock-wave geometry as in the previously discussed examples. The value of γ was the same, also, but several values of M_{∞} were chosen to study the effect of Mach number variation on body shape and surface pressure. The results are as might have been expected, namely, that as Mach number is increased the distance between the body and shock wave decreases until eventually the two attain a fixed distance apart. The results of these computations are shown in figures 5 and 6.

Another series of bodies was computed where the shock wave is given by $\theta_o = 30^{\circ}$, $b/a = 0.6$, as before, and for very large Mach number. Several different values of the adiabatic constant γ were chosen and the effect of varying this constant on body shape and surface pressure was observed (see figs. 7 and 8). Values were taken in the range $1.6667 \geq \gamma \geq 1.001$. Note that the distance between shock wave and body decreases until at $\gamma = 1.001$ body and shock are sensibly coincident. The pressure distribution calculated by simple Newtonian theory for a body having the same dimensions as the shock wave of this series is shown in figure 8. It is to be compared with the pressure on the body found here for $\gamma = 1.001$. The difference between the two curves is undoubtedly due to centrifugal effects which cannot be calculated with the Newtonian theory, but which are included in the so-called Newtonian plus centrifugal theory. The latter theory is arrived at by taking γ equal to one along with infinite Mach number.

Comparison With an Approximate Theory

In reference 5 an approximate numerical method is presented for computing supersonic flow past cones without axial symmetry. This method is most accurate when the bodies are nearly circular cones, and has the disadvantage that it can only be applied with ease to cases for which reference 5 presents tabulated coefficients.

To compare the present method with that of reference 5 a tabulated case was found for which the shock wave was very nearly an elliptic cone. The body is a simple perturbation of a 25° circular cone in a flow where $M = 3.926$, $\gamma = 1.405$. The initial shock which produced this body was given by $\theta_o = 30.990^{\circ}$, $b/a = 0.94337$. As the starting condition, the method of reference 5 was applied to the body produced by this calculation, and the shock-wave position and surface pressures were computed. The body was closely approximated by the expression

$$\theta_b = 25 + 1.097 \cos 2\phi \,, \quad \text{degrees} \tag{40}$$

and the shock wave is given by the expression

$$\theta = 31.737 + 0.747 \cos 2\phi \,, \quad \text{degrees} \tag{41}$$

The surface pressure calculated by the method of reference 5 is

$$p_b = 0.2396 + 0.0185 \cos 2\phi \tag{42}$$

A simple analysis of the surface pressure as calculated by the method of the present paper shows that it can be put in the form

$$p_b = 0.2486 + 0.0120 \cos 2\phi \tag{43}$$

The results of these computations are shown in figures 9 and 10. The angles θ and ϕ in equations (40) through (42) are true spherical polar angles, and they belong to the coordinate system of equations (1) when $k^2 = 1$ and $k'^2 = 0$.

The body and shock-wave comparison is very close. The pressures, on the other hand, disagree by as much as 6.5 percent. At least a portion of this difference can be accounted for if one recalls that the problem is in fact highly nonlinear, and that the method of reference 5 is based on linearizing assumptions.

A Limiting Case

When the value of b/a is taken to be unity, the shock wave and resulting body are circular cones. A calculation was made for such a case using $\theta_o = 28.589^{\circ}$, $M = 8.096$, and $\gamma = 1.405$, and using several different values for $\Delta\theta$. The results are shown in the table below. This same case has been tabulated in reference 4, and for purposes of comparison the reference 4 results are also given in the table. Note that the results of the two methods of computation are nearly identical for the smaller values of $\Delta\theta$.

	$\Delta\theta = 1^\circ$	$\Delta\theta = 0.5^\circ$	$\Delta\theta = 0.25^\circ$	$\Delta\theta = 0.125^\circ$	Ref. 4
ρ_o/ρ_∞	4.4681	4.4681	4.4681	4.4681	4.4682
p_o/p_∞	17.367	17.367	17.367	17.367	17.369
p_b/p_o	1.0847	1.0764	1.0718	1.0696	1.0673
ρ_b/ρ_∞	1.0594	1.0538	1.0507	1.0489	1.0474
θ_b	25.028°	25.014°	25.007°	25.004°	25.000°

DISCUSSION OF RESULTS

In the foregoing section the effect on body shape and surface pressure due to changing the size of the increment $\Delta\theta$ was studied. It was found that the numerical process is convergent in the cases studied. No numerical difficulties were encountered in obtaining these results. The same computing program could not be used for cases where the resulting body was markedly different from a coordinate cone. Such situations arise when the ratio b/a at the shock is smaller than about 0.5, or for Mach numbers smaller than about 4. In the latter case, if the ratio b/a at the shock wave is not too far from unity, then the low Mach number cases can be computed with no difficulty. There are apparently two factors which contribute to these problems. One is the inability to come sufficiently close to the body over the full range $0 \leq \phi \leq 90^\circ$ in such cases, and the other is the more involved matter associated with the entropy layer and singularities on the surface of the body.

Extensions of this work would clearly involve modifying the computing process to minimize the difficulties discussed in the foregoing paragraph. Changes to include angles of attack might also be included. It is likely that considerable information relative to the entropy layer and singularities on the body could be obtained from examination of the region near the body more closely than is possible with the present procedure.

Ames Research Center
National Aeronautics and Space Administration
Moffett Field, Calif., Apr. 20, 1959

REFERENCES

1. Van Dyke, Milton D.: The Supersonic Blunt-Body Problem - Review and Extension. Jour. Aero/Space Sci., vol. 25, no. 8, Aug. 1958, pp. 485-496.

2. Van Dyke, Milton D., and Gordon, Helen D.: Supersonic Flow Past a Family of Blunt Axisymmetric Bodies. NASA REPORT 1, 1959.

3. Yih, Chia-Shun: Stream Functions in Three-Dimensional Flows. Reprint No. 158, State Univ. of Iowa, Reprints in Engineering, July-August, 1957.

4. Staff of the Computing Section (under the direction of Zdeněk Kopal): Tables of Supersonic Flow Around Cones. Tech. Rep. 1, Center of Analysis, M.I.T., Cambridge, 1947.

5. Ness, Nathan, and Kaplita, Thaddeus T.: Tabulated Values of Linearized Conical Flow Solutions for Solution of Supersonic Conical Flows Without Axial Symmetry. PIBAL Rep. No. 220, Polytechnic Institute of Brooklyn, Dept. of Aero. Eng. and Appl. Mech., Jan. 1954.

6. Ferri, Antonio: Supersonic Flow Around Circular Cones at Angles of Attack. NACA Rep. 1045, 1951. (Supersedes NACA TN 2236)

7. Radhakrishnan, G.: The Exact Flow Behind a Yawed Conical Shock. Rep. No. 116, The College of Aeronautics, Cranfield, April, 1958.

8. Holt, M.: A Vortical Singularity in Conical Flow. Quart. Jour. Mech. and Appl. Math., vol. VII, pt. IV, Dec. 1954, pp. 438-445.

9. Kraus, L.: Diffraction by a Plane Angular Sector. Ph. D. Thesis, New York Univ., May 1955.

10. Ames Research Staff: Equations, Tables, and Charts for Compressible Flow. NACA Rep. 1135, 1953.

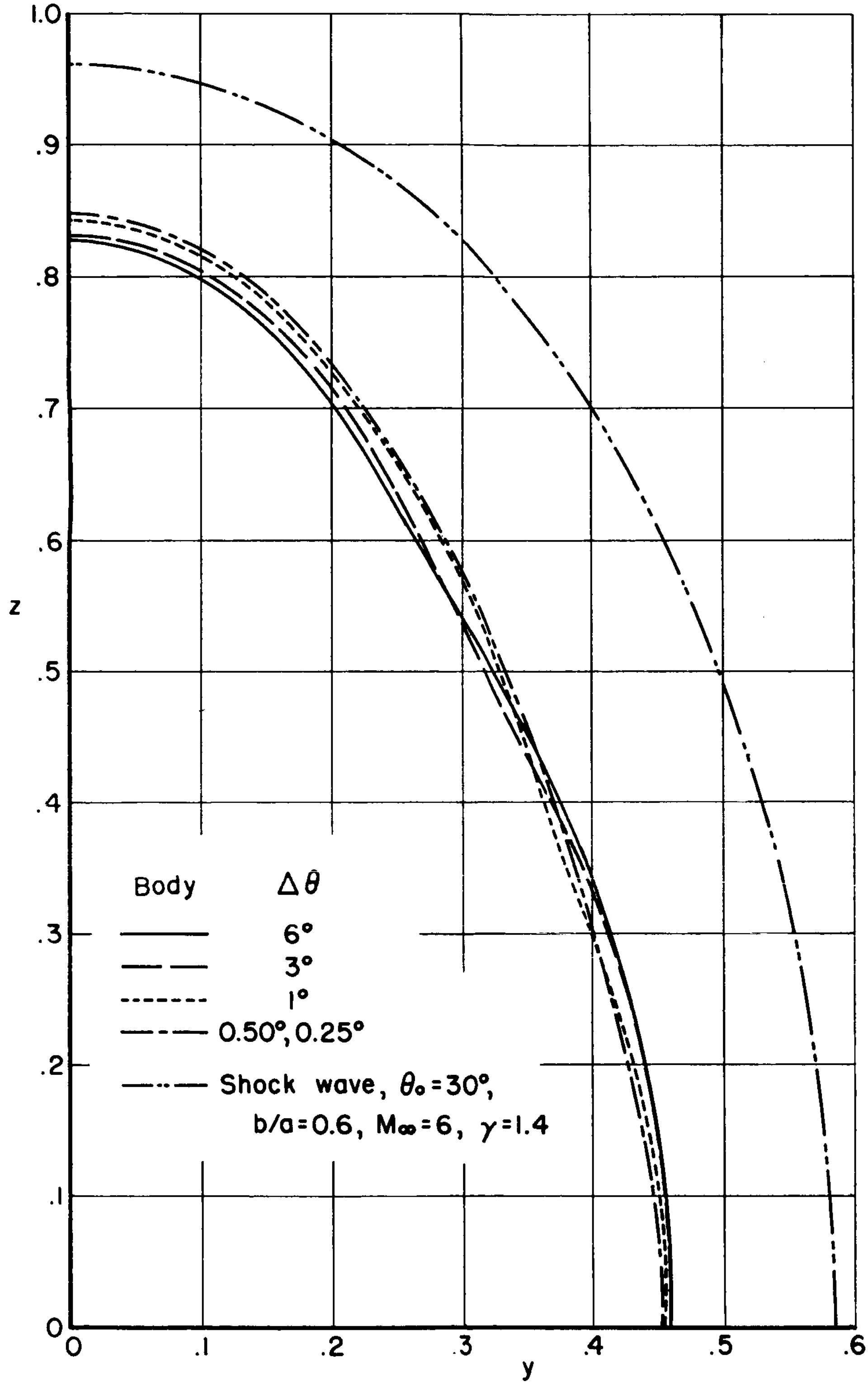

Figure 1.- The effect of mesh size on body shape for a typical case.

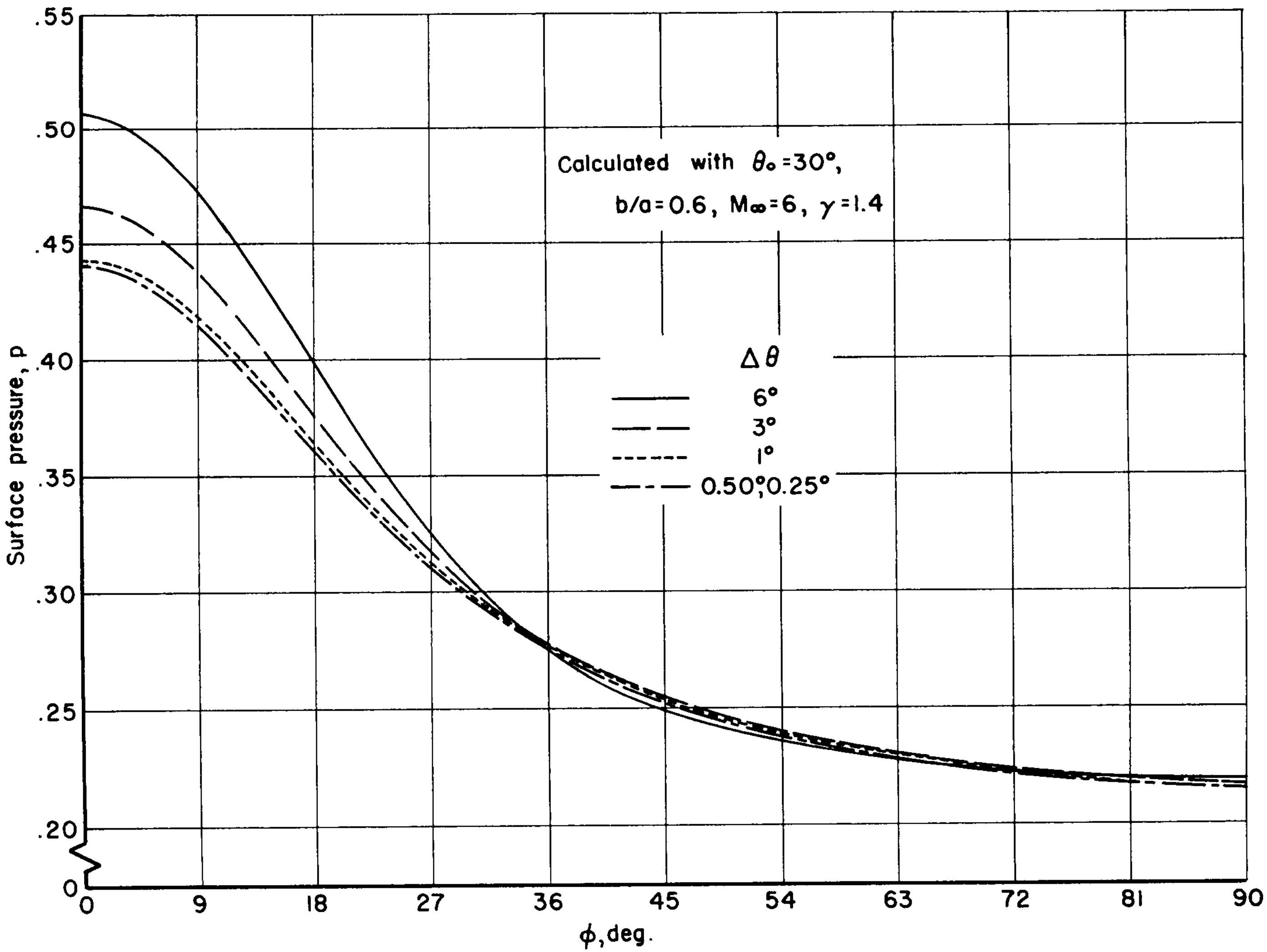

Figure 2.- The effect of mesh size on surface pressure for a typical case.

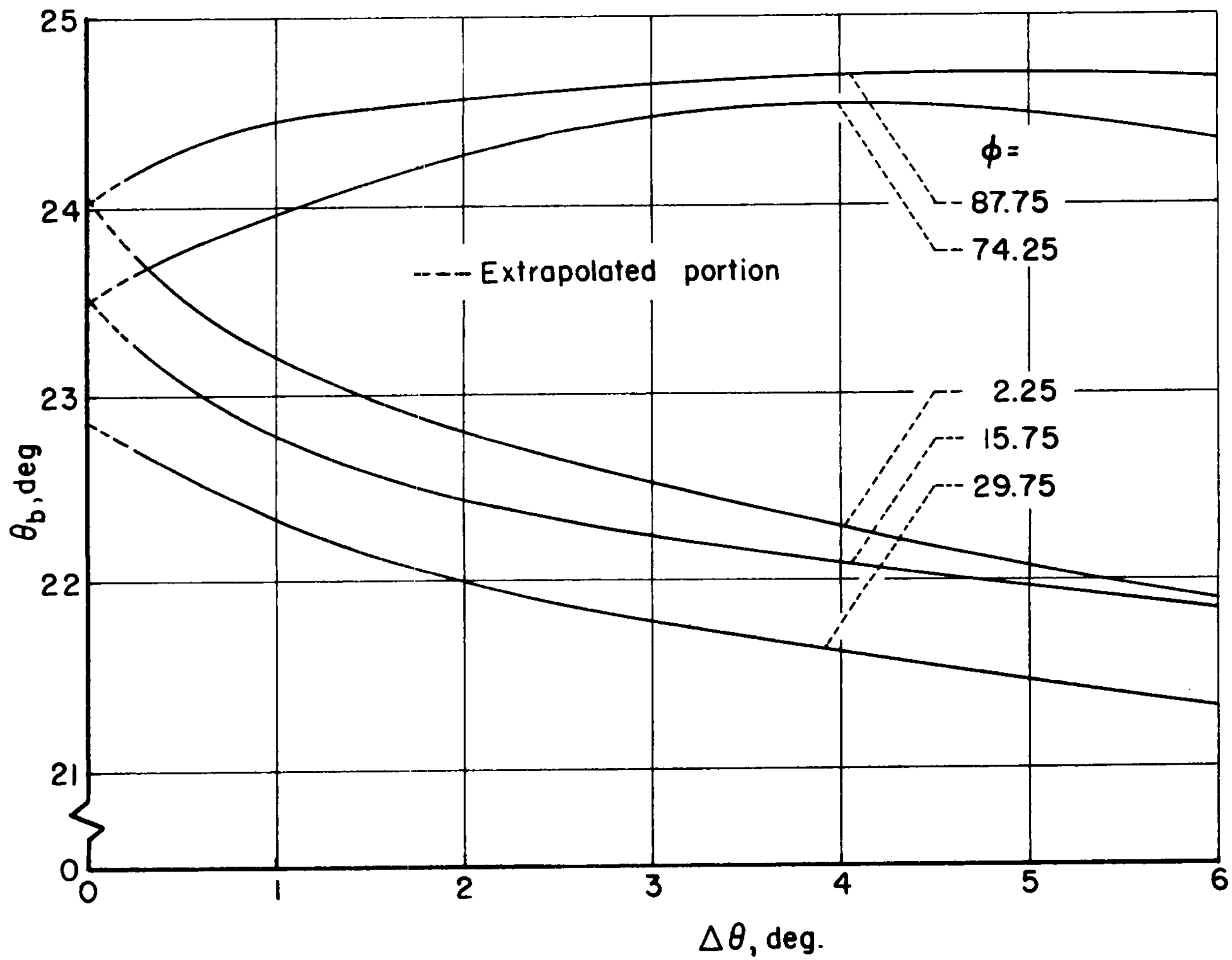

Figure 3.- Variation of the body coordinate θ_b with mesh size $\Delta\theta$ for a typical case having $\theta_o = 30^o$, $b/a = 0.6$, $M_\infty = 6$, $\gamma = 1.4$.

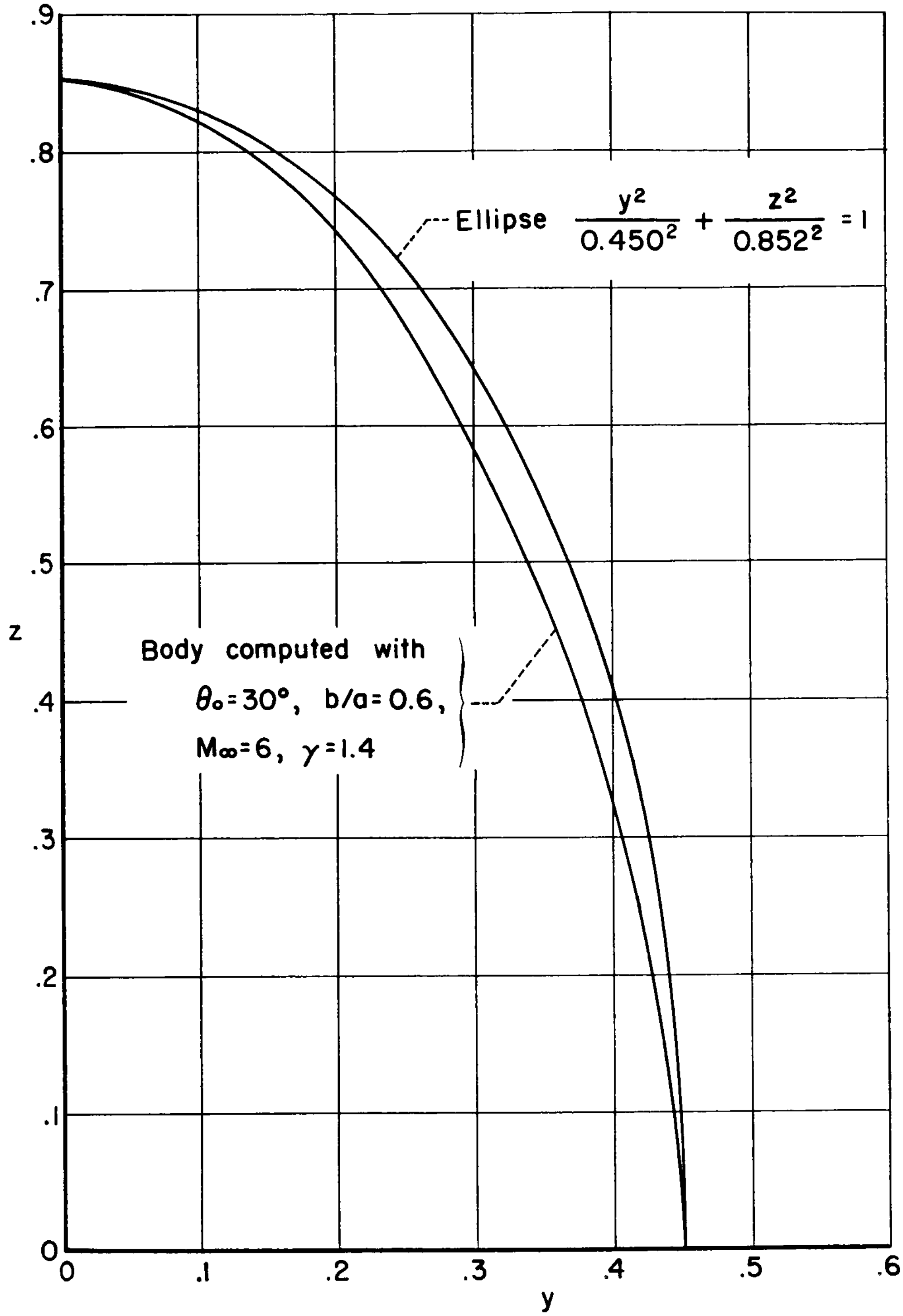

Figure 4.- Comparison of body shape with an ellipse.

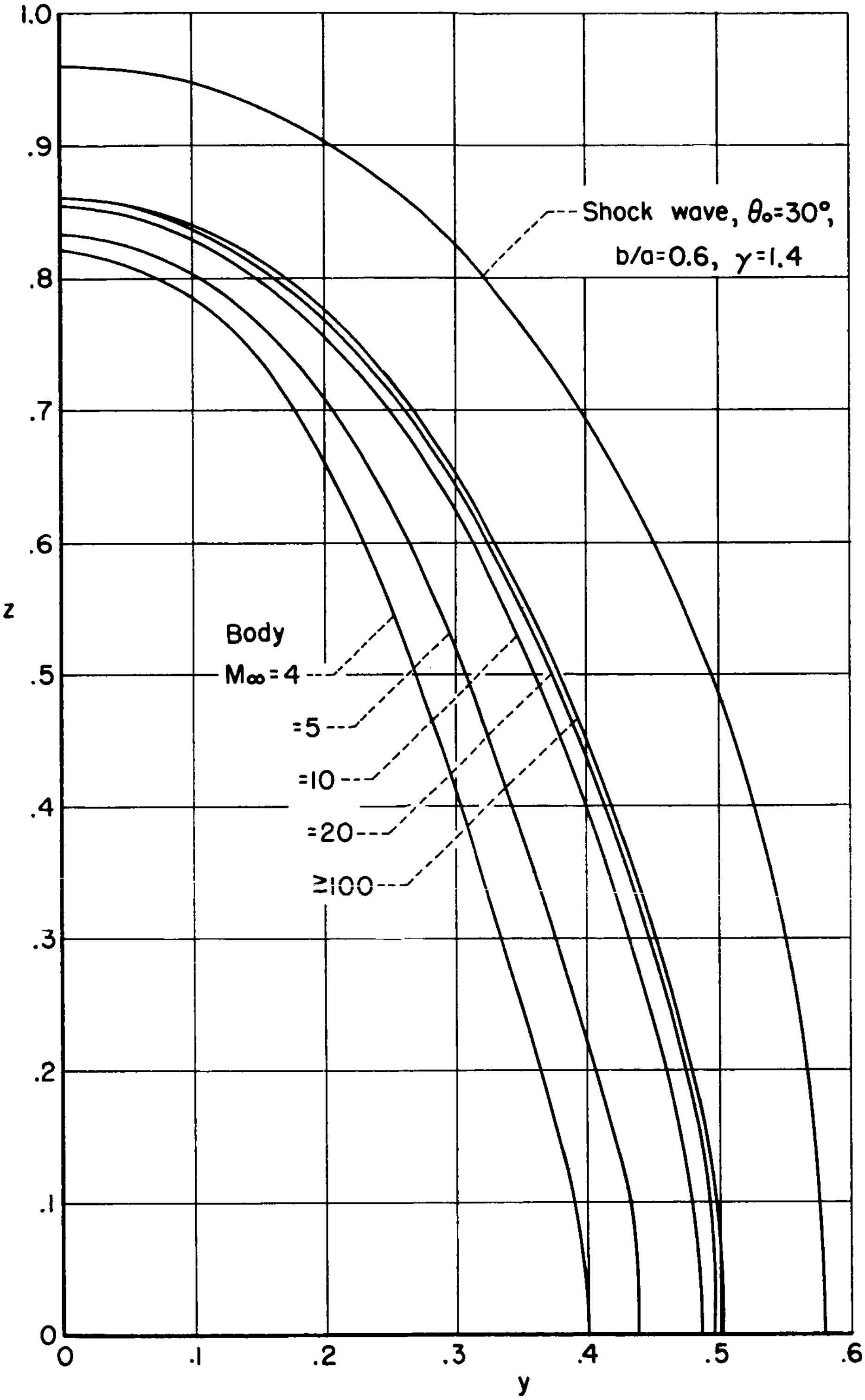

Figure 5.- The effect of Mach number variation on body shape; $\Delta\theta = 1^\circ$.

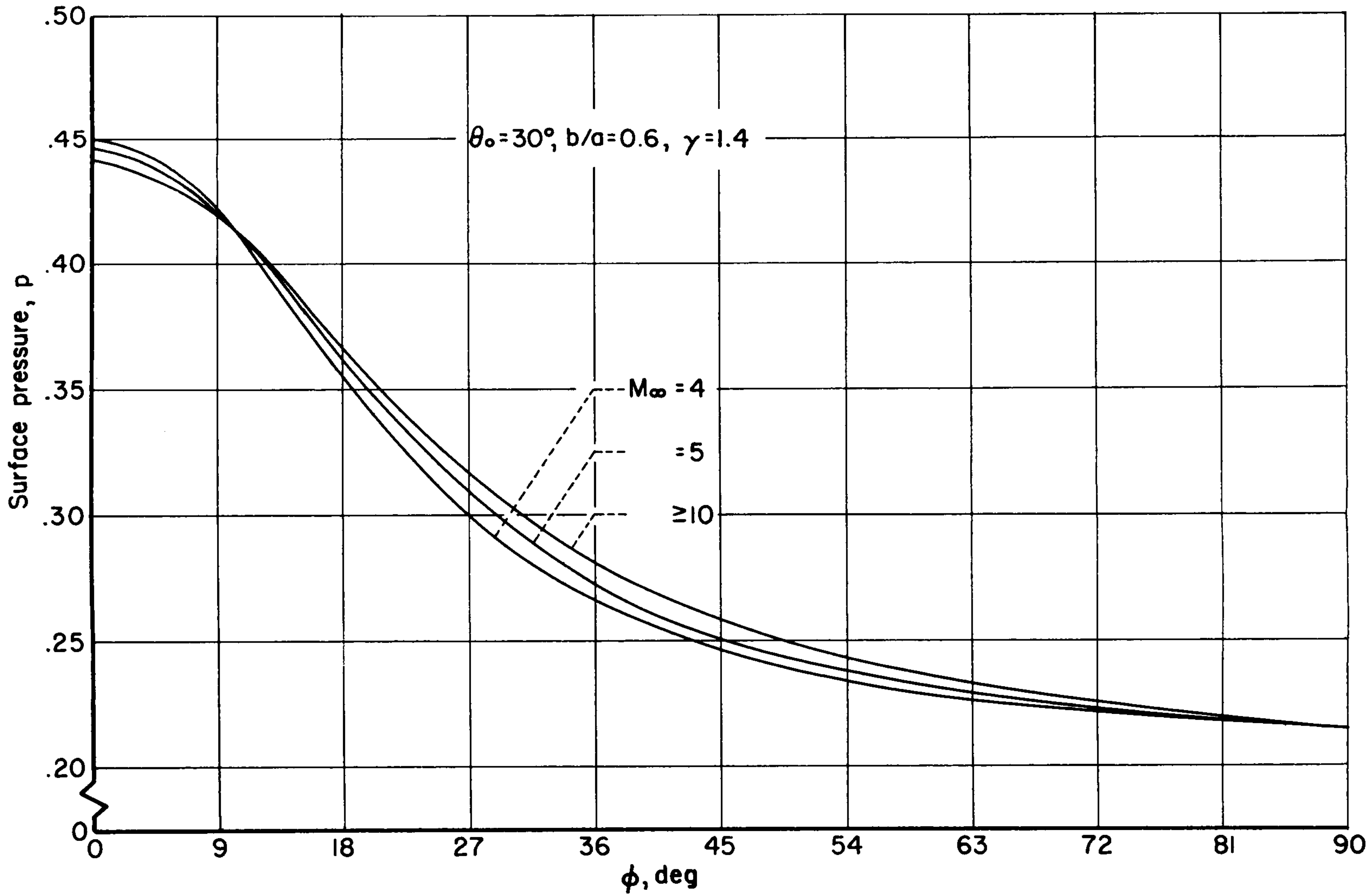

Figure 6.- The effect of Mach number variation on surface pressure; $\Delta\theta = 1^{\circ}$.

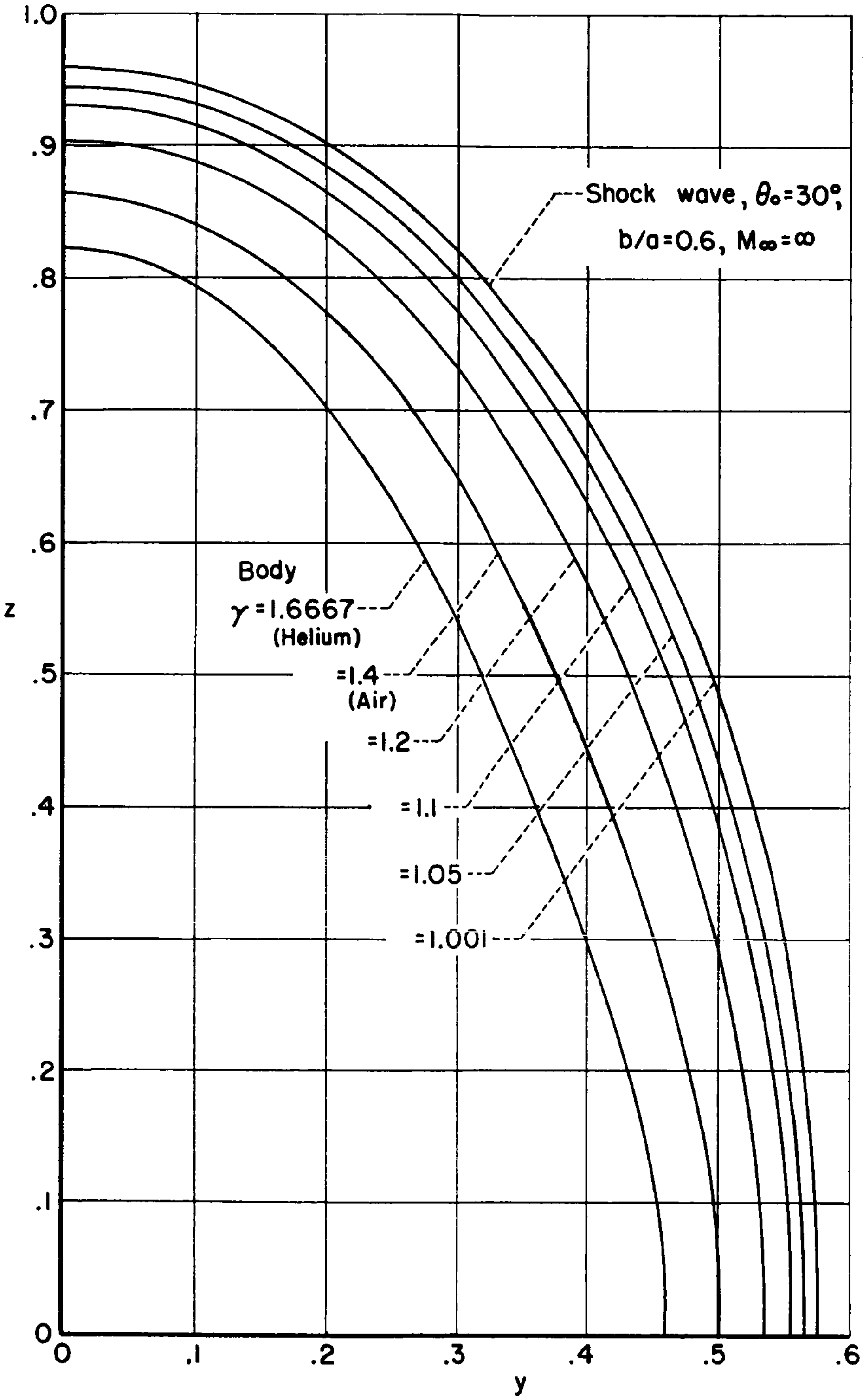

Figure 7.- The effect of changing γ on body shape.

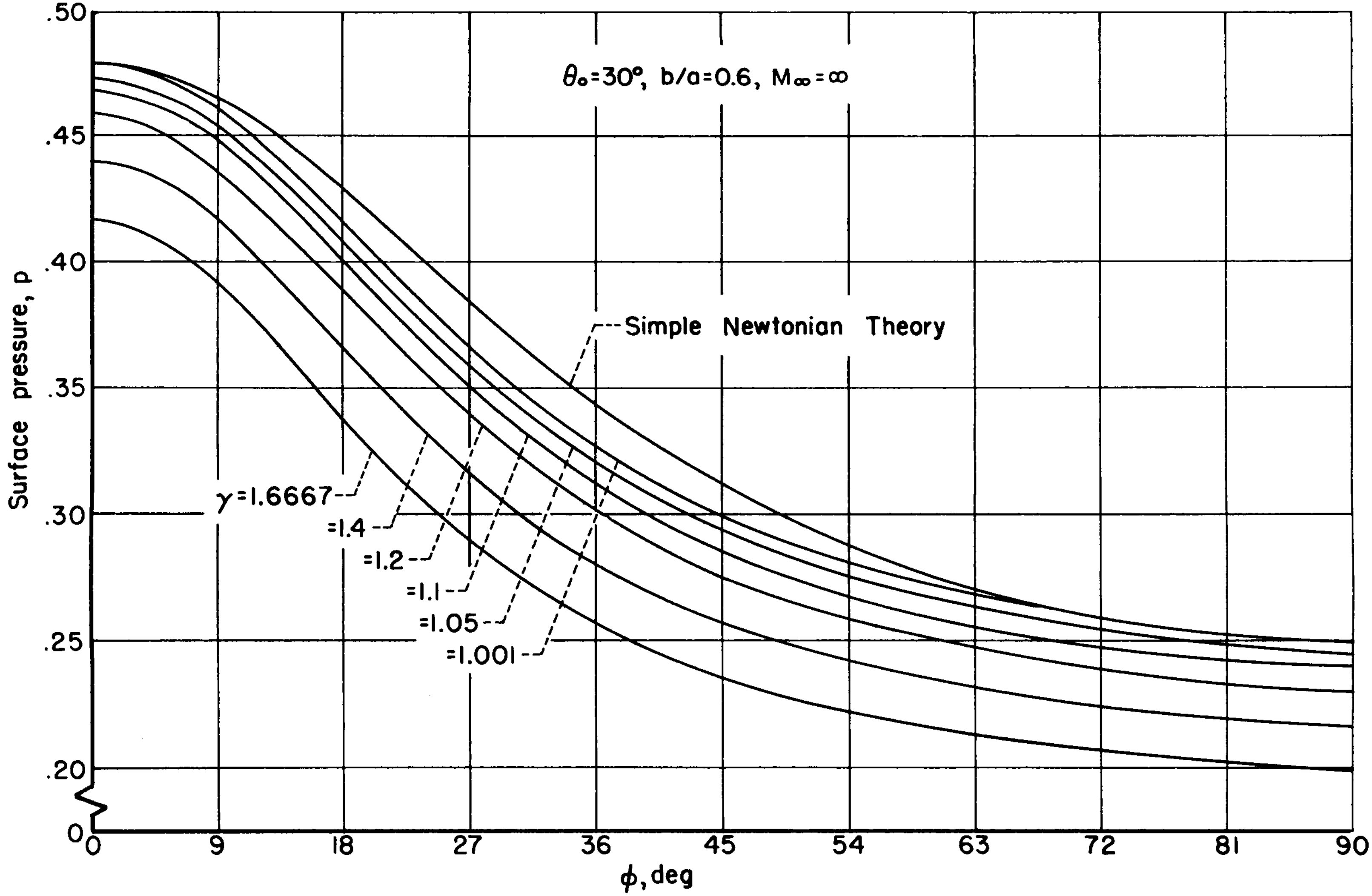

Figure 8.- The effect of changing γ on surface pressure.

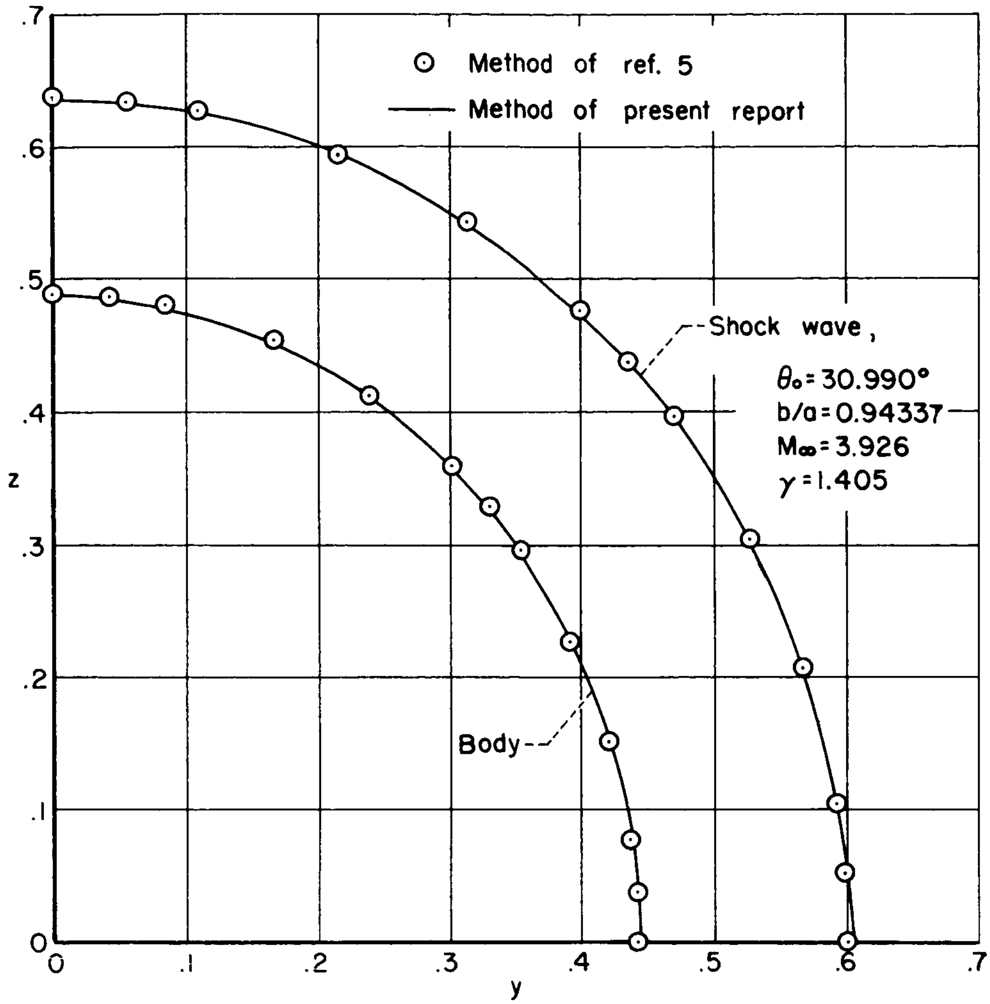

Figure 9.- Comparison of shock and body shapes.

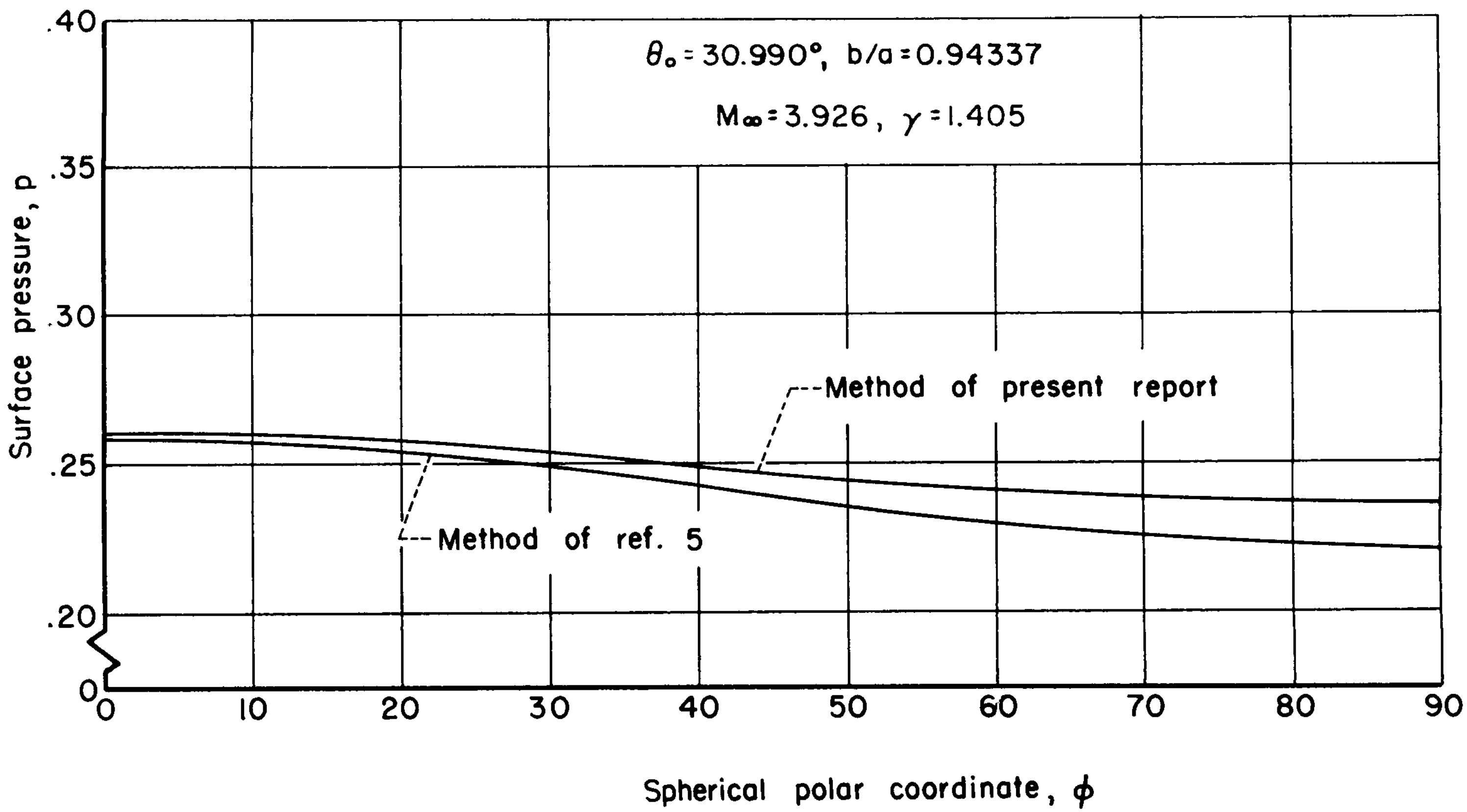

Figure 10.- Comparison of surface pressures.